ARTICLE

CHRONIC MYELOPROLIFERATIVE NEOPLASMS

SRSF2-P95H decreases JAK/STAT signaling in hematopoietic cells and delays myelofibrosis development in mice

Christophe Willekens[1,2,3], Lucie Laplane[1,4], Tracy Dagher[1,2], Camelia Benlabiod[1,2,4], Nicolas Papadopoulos[5,6], Catherine Lacout[1], Philippe Rameau[7], Cyril Catelain[7], Alexia Alfaro[7], Valérie Edmond[1], Nicolas Signolle[7], Valentine Marchand[1,2], Nathalie Droin[1,2,7], Remco Hoogenboezem[8], Rebekka K. Schneider[8,9], Alex Penson[10], Omar Abdel-Wahab[10], Stephane Giraudier[11], Florence Pasquier[1,3], Caroline Marty[1,2], Isabelle Plo[1,2], Jean-Luc Villeval[1,2], Stefan N. Constantinescu[5,6,12,13], Françoise Porteu[1,2], William Vainchenker[1,2] and Eric Solary[1,2,3]✉

Heterozygous mutation targeting proline 95 in Serine/Arginine-rich Splicing Factor 2 (SRSF2) is associated with V617F mutation in Janus Activated Kinase 2 (JAK2) in some myeloproliferative neoplasms (MPNs), most commonly primary myelofibrosis. To explore the interaction of *Srsf2*^{P95H} with *Jak2*^{V617F}, we generated Cre-inducible knock-in mice expressing these mutants under control of the *stem cell leukemia (Scl)* gene promoter. In transplantation experiments, *Srsf2*^{P95H} unexpectedly delayed myelofibrosis induced by *Jak2*^{V617F} and decreased TGFβ1 serum level. *Srsf2*^{P95H} reduced the competitiveness of transplanted *Jak2*^{V617F} hematopoietic stem cells while preventing their exhaustion. RNA sequencing of sorted megakaryocytes identified an increased number of splicing events when the two mutations were combined. Focusing on JAK/STAT pathway, *Jak2* exon 14 skipping was promoted by *Srsf2*^{P95H}, an event detected in patients with *JAK2*^{V617F} and *SRSF2*^{P95} co-mutation. The skipping event generates a truncated inactive JAK2 protein. Accordingly, *Srsf2*^{P95H} delays myelofibrosis induced by the thrombopoietin receptor agonist Romiplostim in *Jak2* wild-type animals. These results unveil *JAK2* exon 14 skipping promotion as a strategy to reduce JAK/STAT signaling in pathological conditions.

Leukemia; https://doi.org/10.1038/s41375-023-01878-0

INTRODUCTION

Myeloproliferative neoplasms (MPNs) are clonal diseases arising from a single, somatically mutated, hematopoietic stem cell (HSC) [1]. One of these diseases is Myelofibrosis (MF), which is characterized by reticulin deposition and fibrosis, resulting in the progressive development of ineffective hematopoiesis, and a propensity for transformation to acute myeloid leukemia [2]. MF development involves the reprogramming of nonhematopoietic mesenchymal stromal lineage cells into fibrosis-driving myofibroblasts [3–5]. The release of fibrogenic soluble mediators by malignant haematopoietic cells mediates this reprogramming. A master soluble mediator in this crosstalk is transforming growth factor beta 1 (TGFβ1) released by abnormal megakaryocytes [6–8].

The most frequent driver event identified in Philadelphia negative MPN is *JAK2*^{V617F}, a gain of function mutation in *JAK2* [1]. MF is typically associated with additional somatic events that may arise before or after the acquisition of *JAK2*^{V617F} [9]. Mouse models have depicted a synergistic contribution of gene deletion affecting the histone methyltransferase *Ezh2* (enhancer of zeste homolog 2) [10–12] or the chromatin modifier *Asxl1* (additional sex combs-like 1) [13] or the DNA methyltransferase *Dnmt3A* [14] to *Jak2*^{V617F}-driven MF development. In contrast, the cooperation between somatic mutation in *Jak2*^{V617F} and the monoallelic somatic mutation affecting proline 95 residue in the splicing factor SRSF2 (serine/arginine-rich splicing factor 2) [15], a key protein of the spliceosome machinery, remains poorly explored. Among MPNs, somatic mutation in *SRSF2*^{P95} was associated with MF features and was suggested to reduce survival [9, 16, 17]. However, while *ASXL1* and *EZH2* mutations are enriched when progressing from pre-fibrotic to fibrotic MPN, this is not observed with *SRSF2*^{P95} that rather correlates with an increased risk of leukemic transformation [9, 18, 19].

[1]INSERM U1287, Gustave Roussy Cancer Campus, Villejuif, France. [2]Faculté de Médecine, Université Paris-Saclay, Le Kremlin-Bicêtre, France. [3]Département d'hématologie, Gustave Roussy Cancer Campus, Villejuif, France. [4]Institut d'Histoire et Philosophie des Sciences et des Techniques, Université Paris I Panthéon-Sorbonne, Paris, France. [5]Ludwig Institute for Cancer Research Brussels, Brussels, Belgium. [6]Université catholique de Louvain and de Duve Institute, Brussels, Belgium. [7]Gustave Roussy Cancer Campus, Villejuif, France. [8]Department of Hematology, Erasmus University, Rotterdam, The Netherlands. [9]Department of Hematology, Oncology, Hemostaseology, and Stem Cell Transplantation, RWTH Aachen University, Aachen, Germany. [10]Human Oncology and Pathogenesis Program, Memorial Sloan Kettering Cancer Center, New York, NY, USA. [11]Hematology department, Saint-Louis Hospital, Paris, France. [12]WELBIO department, WEL Research Institute, Wavre, Belgium. [13]Ludwig Institute for Cancer Research, Nuffield Department of Medicine, Oxford University, Oxford, UK. ✉email: eric.solary@gustaveroussy.fr

Received: 2 December 2022 Revised: 10 March 2023 Accepted: 15 March 2023
Published online: 26 April 2023

To better explore how these two mutational events interact in hematopoietic cells, we crossed Cre-inducible *Jak2*$^{VF/+}$ [20] and *Srsf2*$^{P95H,/+}$ [21] knock-in mouse models under *Scl (stem cell leukemia)* gene promoter. Our results reveal the attenuation of *Jak2*^{V617F}-induced phenotype by *Srsf2*^{P95H} that delays MF development while preventing *Jak2*^{V617F} HSC exhaustion. One of the pre-mRNA splicing events amplified by *Srsf2*^{P95H} is the skipping of *Jak2* exon 14 in hematopoietic stem and progenitor cells (HSPCs), generating an inactive protein that may contribute to the downregulation of JAK-STAT signaling in these cells.

METHODS

Animal models

Transgenic mice expressing a Cre-recombinase–inducible *Jak2*^{V617F} [20] were crossed with transgenic mice expressing a Cre-recombinase-inducible *Srsf2*^{P95H} [21] to generate double-mutant mice on a C57BL/6 background (Supplementary Fig. 1A). Single and double transgenic animals were crossed with animals expressing the tamoxifen-inducible Cre-ER(T) recombinase under the control of the stem cell leukemia (*Scl*) locus enhancer (herein referred to as *Scl-Cre*^{ERt} transgenic animals) [22] to generate offsprings in which tamoxifen gavage could trigger the expression of heterozygous *Jak2*^{V617F}, heterozygous *Srsf2*^{P95H} or the two mutated alleles. In transplant experiments, recipient mice were 8-week old C57BL/6 females (Envigo Labs, www.envigo.com) intravenously engrafted with 3×10^6 bone marrow cells after lethal irradiation (9.5 Gy). Recombinase Cre expression was induced 5 weeks after transplantation by tamoxifen gavage (500 mg/kg/day for 2 days). Romiplostim-induced myelofibrosis was generated as described [23]. Peripheral blood samples were serially collected on citrate. Sternum and spleen, as well as bone marrow cells, were collected at sacrifice. Detailed analyses are described in Supplementary Data.

TGFβ1 quantification

Whole peripheral blood was obtained at sacrifice through cardiac puncture and centrifuged at 2200 rpm for 20 min before collecting the serum that was aliquoted and stored at −80 °C. TGF-β1 was measured in duplicates using ELISA on EnSpire Multimode Plate Reader from PerkinElmer.

Flow cytometry

After red blood cell lysis and, when indicted, specific cell sorting, cell suspensions were labeled with indicated antibodies and analyses were performed on LSR Fortessa (BD) and analyzed using Kaluza Analysis software (Beckman Coulter). Ploidy was measured in CD41$^+$ CD42$^+$ cells (see Supplementary Data for details).

Transmission electron microscopy

Bone marrow carrots were fixed in 2% glutaraldehyde in 0.1 M phosphate buffer and were postfixed with 2% osmium tetroxide in 0.1 M phosphate buffer, embedded in Epon™ 812. Polymerization before generating 1 µm semi-thin sections that were stained with standard uranyl acetate and lead citrate and observed with FEI Tecnai 12 electron microscope (FEI, Eindhoven, Netherlands). Digital images were taken using a SIS MegaviewIII CCD camera (Olympus, Tokyo, Japan). Details are provided in Supplementary Data.

RNA sequencing

Bone marrow cells were collected from recipient mice 8–12 weeks after tamoxifen feeding. Lin$^-$ cells were enriched before collecting CD41$^+$ CD42d$^+$ megakaryocytes in Trizol LS (Thermo Fisher, Scientific, www.thermofisher.com/fr) by using Influx 5 laser BD cell sorter. Paired end sequencing of total RNA was performed on Illumina Novaseq. Analysis of differentially expressed genes (DEGs) was performed after correction of batch effects and discarding of low-expressed genes. Details are provided in Supplementary Data. Splicing defects were identified with rMATS v4.1.0 (https://www.pnas.org/content/111/51/E5593) using the Ensembl GRCm38 release 101 annotation. Reads that do not cross an exon boundary were used as well as reads that span junctions. SSNG_score was calculated for each exon by the sum of: +1 for each CCNG, +0.5 for each GCNG, 0.5 for each CGNG and −1 for each GGNG. This is multiplied by 4 (the number of bases in the motif) and divided by the length of the exon to give the SSNG fraction.

Real-time quantitative polymerase chain reaction

Mouse megakaryocytes RNA (100 ng) was reverse transcribed using SuperScript™ IV VILO Master mix with ezDNase enzyme (Thermo Fisher Scientific). RT-qPCR was performed with AmpliTaq Gold polymerase. Jak2 exon14 skipping (NM_008413) was analyzed using Jak2_e13_F: 5′-CTAGATAAAGCACATAGGAACTATTCA-3′ and Jak2_e15_R: 5′CTTCAGGTATGTATCCAGTGATCCAA-3′ primer set. In patients samples, RT-qPCR was performed in sorted granulocytes using JAK2_e13_F: 5′-CGGTCAACTGCATGAAACAGA-3′ and JAK2_ex15_R: 5′-CCAAATTTTACAAACTCCTGAACCAGAAT-3′ (NM_004972) primers. Melting curve profiles were used to visualize exon-14 skipping and the amplicons were separated in a 2% agarose gel (More details in Supplementary Data).

Dual luciferase transcriptional assay

Full-length human *JAK2* cDNA and *JAK2*$^{\Delta ex14}$ cDNA were amplified by PCR and introduced into pCDNA3.1 vector using TOPO Expression Kit (Invitrogen). STAT5 transcriptional activity of these constructs was measured in JAK2-deficient γ−2A cells (mutant gamma1A fibrosarcoma cells) by dual luciferase assay as described [24]. γ-2A cells were transiently transfected using Lipofectamine 3000 (ThermoFisher) with cDNAs coding the SpiLuc reporter as a readout of STAT5 transcriptional activation and pRLTK-Luc reporter as an internal control (Promega) together with human thrombopoietin receptor MPL, murine STAT5 and pcDNA3 vectors encoding or not JAK2 constructs. Medium was changed 4 h after transfection and cells were stimulated or not with 10 ng/mL thrombopoietin (Miltenyi Biotec) for 24 h.

Phosphoflow assay

Mouse BM and spleen Lin$^-$ cells were negatively sorted using rat antibodies targeting Ter-119, B220, Gr-1, CD3 and CD11b and fixed with 1.6% formaldehyde (ThermoFisher). LSK cells were stained with anti-Sca-1 (PE-Cy7) and c-Kit (PE) antibodies (BioLegend), and megakaryocytes with Abs against CD41 (Alexa Fluor 700) and CD42d (APC) (BioLegend). After methanol permeabilization and staining for p-STAT5 (BV421, BD Biosciences), samples were analyzed by flow cytometry (LSRFortessa) with BD FACSDiva software. Data were analyzed with Kaluza Analysis software (Beckman Coulter).

Statistical analysis

Results are shown as means ± SEM. To assess the statistical significance among individual cohorts, one-way ANOVA with subsequent Bonferroni's post-hoc multiple comparison test or unpaired Student's *t* test were used (Prism version 7 software; GraphPad Software). $P \le 0.05$ was considered significant. In all figures, *$P < 0.05$; **$P < 0.01$; ***$P < 0.001$; ****$P < 0.0001$.

Study approval

Animal experiments were conducted in Gustave Roussy animal facility and approved by the ethical review board (#2016–104-7171). All mice were kept under specific pathogen–free conditions with free access to food and water, housed under 12-h light/12-h dark cycles, with monitored ambient temperature (21 ± 1 °C) and humidity range (20–70%), in accordance with French laws for animal welfare. Patient samples were collected samples with informed consent and all authorizations (IRB 00003835-Protocol 2015/59-NICB; CNIL #915663).

RESULTS

Srsf2^{P95H} delays *Jak2*^{V617F}-induced myelofibrosis

Since *Scl*-promoter driven genes are expressed in both hematopoietic and endothelial cells, we engrafted bone marrow cells collected from *Scl-Cre*^{ERt}-*Srsf2*^{P95H}, *Scl-Cre*^{ERt}-*Jak2*^{V617F}, *Scl-Cre*^{ERt}-*Jak2*^{V617F}/*Srsf2*^{P95H}, and *Scl-Cre*^{ERt} (control) animals into lethally irradiated congenic recipient animals and tamoxifen was given five weeks after transplantation, which allowed to specifically explore gene expression impact on hematopoietic cells (Supplementary Fig. 1A and Fig. 1A). Sequential peripheral blood analyses showed an increase in hemoglobin level (Supplementary Fig. 1B), white blood cell count (Supplementary Fig. 1C) and platelet count (Fig. 1B) two weeks after tamoxifen gavage in *Jak2*^{V617F} expressing animals. The increase in hemoglobin level and white blood cell count was initially slowed down by *Srsf2*^{P95H} co-mutation

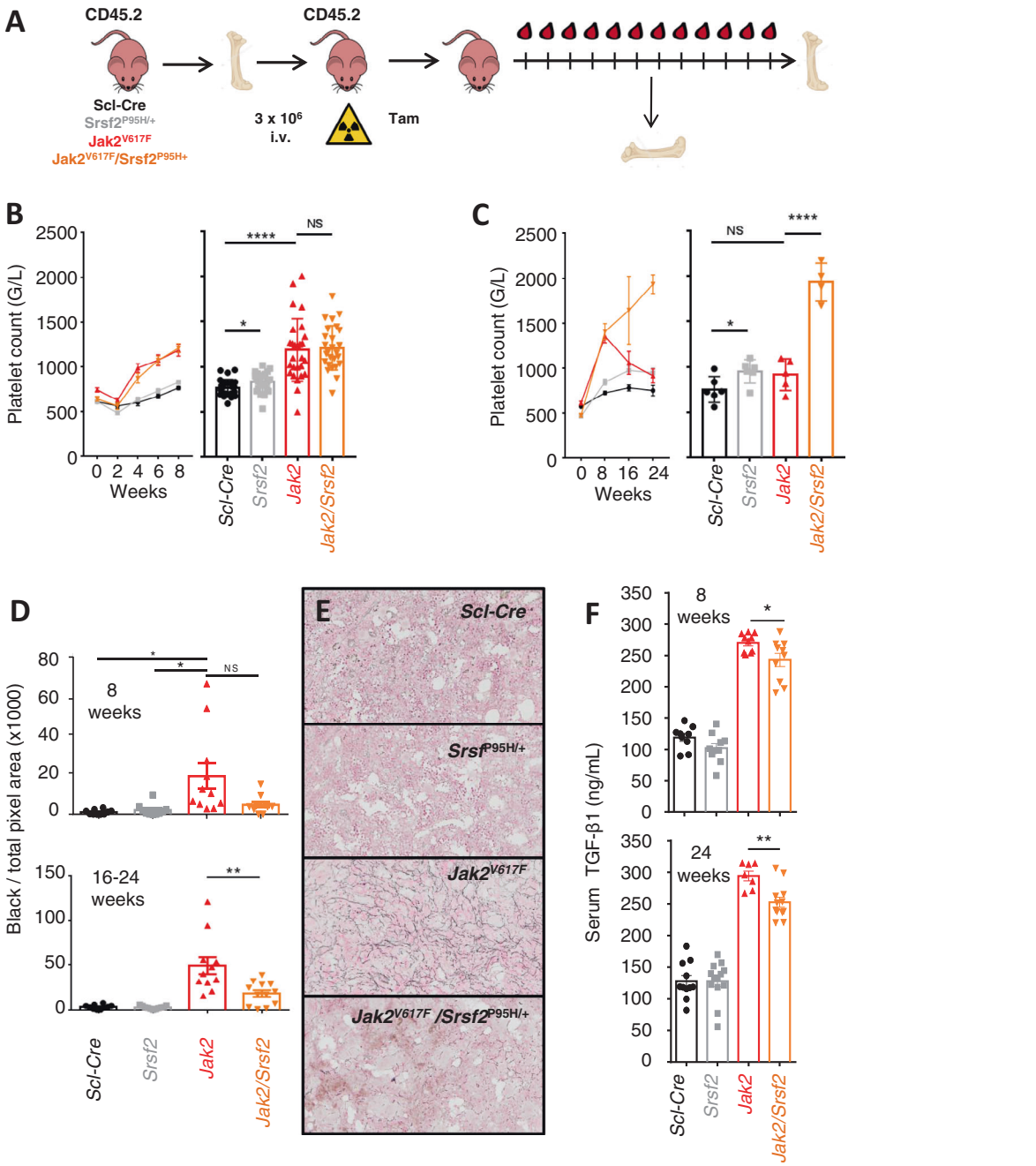

Fig. 1 Co-mutation of *Srsf2*^{P95H} delays *Jak2*^{V617F}-induced myelofibrosis. A Bone marrow cells (3×10^6) from *Scl-Cre* mice, either crossed or not with knock-in mice for *Srsf2*^{P95H}, *Jak2*^{V617F} or the two mutated alleles, were engrafted into lethally irradiated congenic recipients, 5 weeks before tamoxifen gavage. Phlebotomies (180 µL) were performed every 2 weeks for up to 14 weeks to prevent premature death of *Jak2*^{V617F} animals. **B**, **C** Peripheral blood platelet count at indicated time points after tamoxifen gavage (left panels) and at 8 weeks post-tamoxifen (right panels); **B** three independent experiments are pooled; mean ± SEM of *Scl-Cre* ($n = 25$), *Srsf2*^{P95H} ($n = 26$), *Jak2*^{V617F} ($n = 27$), *Jak2*^{V617F}/*Srsf2*^{P95H} ($n = 26$); **C** one experiment, mean ± SEM of *Scl-Cre* ($n = 5$), *Srsf2*^{P95H} ($n = 6$), *Jak2*^{V617F} ($n = 5$), *Jak2*^{V617F}/*Srsf2*^{P95H} ($n = 4$). **D** Bone marrow reticulin fibrosis quantified by computer-assisted imaging, 8 and 16–24 weeks after tamoxifen gavage. Results collected from 2 independent experiments, mean ± SEM of *Scl-Cre* ($n = 10$), *Srsf2*$^{P95H/+}$ ($n = 10$), *Jak2*^{V617F} ($n = 11$), *Jak2*^{V617F}/*Srsf2*$^{P95H/+}$ ($n = 10$) per group; **E** Representative reticulin fiber staining (Gordon and Sweet's and von Willebrand Factor staining) in bone marrow examined 24 weeks after tamoxifen from indicated genotypes (magnification × 25). **F** Serum concentration of TGFβ1 measured by ELISA 8 weeks (upper panel) and 24 weeks (lower panel) after tamoxifen. *Scl-Cre* ($n = 11$), *Srsf2*$^{P95H/+}$ ($n = 13$), *Jak2*^{V617F} ($n = 7$), *Jak2*^{V617F} *Srsf2*$^{P95H/+}$ ($n = 12$). Statistical analyses, unpaired t-test, *$P < 0.05$; **$P < 0.01$; ****$P < 0.0001$, NS not significant.

(Supplementary Fig. 1B, C), with *Srsf2*^{P95H} mostly decreasing B220$^+$ B-cell number among white blood cells (Supplementary Fig. 1D), as previously described in *Srsf2*$^{P95H/+}$ animals [21]. Within the first 8 weeks after tamoxifen gavage, *Jak2*^{V617F} -induced thrombocytosis was not affected by *Srsf2*^{P95H} (Fig. 1B). At later time points, the platelet count decreased in *Jak2*^{V617F} but continued to rise in animals co-expressing *Srsf2*^{P95H} (Fig. 1C).

BM histopathology detected an increase in reticulin fibrosis in animals expressing *Jak2*^{V617F} in hematopoietic cells, eight weeks after initiation of tamoxifen gavage (Supplementary Fig. 1E), which

further increased with time (Fig. 1D). Fibrosis was significantly delayed by *Srsf2*^{P95H} co-expression (Fig. 1D, E). At 8 and 24 weeks after tamoxifen gavage, *Srsf2*^{P95H} also reduced *Jak2*^{V617F}-induced splenomegaly and spleen fibrosis (Supplementary Fig. 1F) as well as the twofold increase in the serum level of TGFβ1 induced by *Jak2*^{V617F} (Fig. 1G). Together, these experiments provided the unexpected observation that the co-expression of *Srsf2*^{P95H} in mouse hematopoietic cells delays rather than promotes *Jak2*^{V617F} induced myelofibrosis.

Srsf2^{P95H} delays exhaustion of *Jak2*^{V617F} stem cells in stressful conditions

We analyzed HSPCs in the BM and spleen of transplanted mice between 16 and 24 weeks after tamoxifen gavage. We observed an increase in the fraction of LSK (Lin$^-$ Sca-1$^+$ Kit$^+$), MPP (LSK CD48$^+$ CD150$^-$) and SLAM (LSK CD48$^-$ CD150$^+$) cells in animals engrafted with either *Jak2*^{V617F} or *Jak2*^{V617F}/*Srsf2*^{P95H} cells when compared to *Scl-Cre* and *Srsf2*^{P95H}, without significant difference between *Jak2*^{V617F} or *Jak2*^{V617F}/*Srsf2*^{P95H} engrafted animals (Fig. 2A).

In competitive experiments, CD45.1 recipient mice were first engrafted with an equal fraction of CD45.2 *Jak2*^{V617F} cells expressing the green fluorescent protein (GFP) and CD45.2 *Jak2*^{V617F}/*Srsf2*^{P95H} GFP-negative cells (Supplementary Fig. 2A). Double-mutant cells demonstrated a decreased competitiveness attested by the reduced fraction of GFP-negative SLAM in the BM (Supplementary Fig. 2B) and the time-dependent decrease in GFP-negative peripheral blood cells (Supplementary Fig. 2C).

We also transplanted CD45.1 recipient animals with 30% genetically modified cells mixed with 70% wild-type cells expressing the GFP (Fig. 2B). In accordance with previous report [19], *Srsf2*^{P95H} alone decreased cell competitiveness in transplanted animals, as indicated by the rapid loss of GFP-negative Ter119$^+$ cells in the peripheral blood. When combined with *Jak2*^{V617F}, *Srsf2*^{P95H} slightly delayed the rapid increase in Ter119$^+$ cells induced by *Jak2*^{V617F} alone (Supplementary Fig. 2D). Analysis of GFP-negative SLAM cells in the BM collected 24 weeks after tamoxifen gavage demonstrated a decrease in the fraction of *Srsf2*^{P95H} cells while *Jak2*^{V617F} cells almost completely invaded the SLAM compartment. *Srsf2*^{P95H} co-mutation significantly reduced *Jak2*^{V617F} SLAM cell expansion (Fig. 2C).

BM cells isolated from these animals were used to perform serial transplantations in recipient CD45.1 animals (Fig. 2D). The third transplantation was associated with a significant decrease in the survival of animals engrafted with *Jak2*^{V617F} compared to *Jak2*^{V617F}/*Srsf2*^{P95H} containing BM cells (Fig. 2E). After this third transplantation, *Srsf2*^{P95H} or *Jak2*^{V617F} SLAM cells had almost disappeared from the BM, contrasting with the expansion of *Jak2*^{V617F}/*Srsf2*^{P95H} double-mutant cells (Fig. 2F), amplifying an effect already observed after the second transplantation (Supplementary Fig. 2E). Finally, monitoring of peripheral blood cells after the third transplantation showed significantly higher white blood cell and platelet counts in mice engrafted with BM cells containing *Jak2*^{V617F}/*Srsf2*^{P95H} compared to *Jak2*^{V617F} alone cells (Fig. 2G). Together, *Srsf2*^{P95H} co-mutation preserved *Jak2*^{V617F} SLAMs from exhaustion in stressful conditions provoked by serial transplantations.

Srsf2^{P95H} interferes with *Jak2*^{V617F}-induced megakaryocyte phenotype

Given their acknowledged role in TGFβ synthesis and MF development, we explored the phenotype of megakaryocytes in transgenic animals. Initial analysis were performed 8 weeks post tamoxifen. We quantified megakaryocytes by von Willebrand factor (vWF) staining of BM sections. *Jak2*^{V617F} induced an increase in the number of BM megakaryocytes as compared to *Scl-Cre* and *Srsf2*^{P95H}-transplanted animals, without significant impact of concomitant *Srsf2*^{P95H} mutation (Fig. 3A). Similarly, electron microscopy did not detect ultrastructural modifications of megakaryocytes according to their mutational status (Supplementary Fig. 3A). *Srsf2*^{P95H} alone or co-expressed with *Jak2*^{V617F} induced a slight decrease in the size of megakaryocytes (Fig. 3B). In agreement with decreased megakaryocyte size, *Srsf2*^{P95H} co-expression with *Jak2*^{V617F} was associated also with a slight decrease in cell ploidy compared to *Jak2*^{V617F} megakaryocytes (Fig. 3C and Supplementary Fig. 3B). The decreased expression of the thrombopoietin receptor MPL typically observed at the surface of *Jak2*^{V617F} cells [25] was also prevented by *Srsf2*^{P95H} co-mutation (Fig. 3D).

At later time points, 16–24 weeks post tamoxifen, the number of megakaryocytes measured in vWF-stained BM remained high in both *Jak2*^{V617F} and *Jak2*^{V617F}/*Srsf2*^{P95H} animals, yet this number had decreased in *Jak2*^{V617F} mice as compared to earlier time points and was still increasing in double-mutant mice (Fig. 3E and Supplementary Fig. 3C). This evolution correlated with platelet count (Fig. 1C), with megakaryocyte erythroid progenitor (MEP) and megakaryocyte progenitor (MKP) fractions in the BM (Supplementary Fig. 3D), and with megakaryocyte ploidy (Fig. 3F). Together, *Srsf2*^{P95H} on its own only slightly decreased megakaryocyte size while it negatively interfered with *Jak2*^{V617F}-induced longitudinal changes in BM megakaryocyte number and maturation.

Srsf2^{P95H} down-regulates cell signaling in megakaryocytes

We sequenced RNA of megakaryocytes enriched from *Scl-Cre*, *Srsf2*^{P95H}, *Jak2*^{V617F} and *Jak2*^{V617F}/*Srsf2*^{P95H} mouse BM samples. Dimensionnality reduction through principal component analysis (PCA) separated megakaryocytes from *Jak2*^{WT} and *Jak2*^{V617F} animals, regardless of the *Srsf2* status (Supplementary Fig. 4A). Pairwise differential analysis consistently showed a high impact of *Jak2*^{V617F} and a more limited impact of *Srsf2*^{P95H} on gene expression (as defined by a Padj <0.05) in megakaryocytes. For example, compared to *Scl-Cre* megakaryocytes, the *Srsf2*^{P95H} mutation changed the expression of 75 genes while *Jak2*^{V617F} mutation, with or without *Srsf2*^{P95H}, altered the expression of about 3000 genes (Supplementary Fig. 4B). The upset plot showed that, among the six pairwise analysis, the largest intersection between differentially expressed genes (DEG) was across samples with *Jak2*^{V617F} mutation (Supplementary Fig. 4C).

Megakaryocytes collected from double-mutant *Jak2*^{V617F} / *Srsf2*^{P95H} mice clustered separately from single mutant *Jak2*^{V617F} cells (Fig. 4A), with 71 DEG between these two conditions (Fig. 4B). Gene set enrichment analysis (GSEA) indicated the downregulation of multiple signaling pathways, including JAK-STAT, TNF and TGFβ signaling pathways, in *Jak2*^{V617F}/*Srsf2*^{P95H} compared to *Jak2*^{V617F} cells (Fig. 4C). Comparison of enrichment scores further confirmed the upregulation of signaling pathways in *Jak2*^{V617F} megakaryocytes and their downregulation in cells expressing *Srsf2*^{P95H}, either alone or with *Jak2*^{V617F} (Fig. 4D). Together, these results indicate that *Srsf2*^{P95H} reduces the enrichment in signaling pathways observed in *Jak2*^{V617F} megakaryocytes.

Srsf2^{P95H}-induced *Jak2* exon 14 skipping

SRSF2 splicing factor recognizes both CCNG and GGNG sequences [26]. Using RNA sequences collected from sorted megakaryocytes, we compared the relative enrichment of all four SSNG variants, where S represents C or G, in cassette exons that were differentially spliced upon expression of mutant *Srsf2*^{P95H}, in the context of either wild-type or mutated *Jak2*. Megakaryocytes expressing *Srsf2*^{P95H} either alone or in combination with *Jak2*^{V617F} exhibited an enrichment for CCNG while the other sequences, especially GGNG, were depleted in exons that were included versus excluded, respectively (Fig. 5A). Based on a False Discovery Rate (FDR) < 0.05, we detected a total number of 1729 differential splicing events in mutated compared to *Scl-Cre* megakaryocytes.

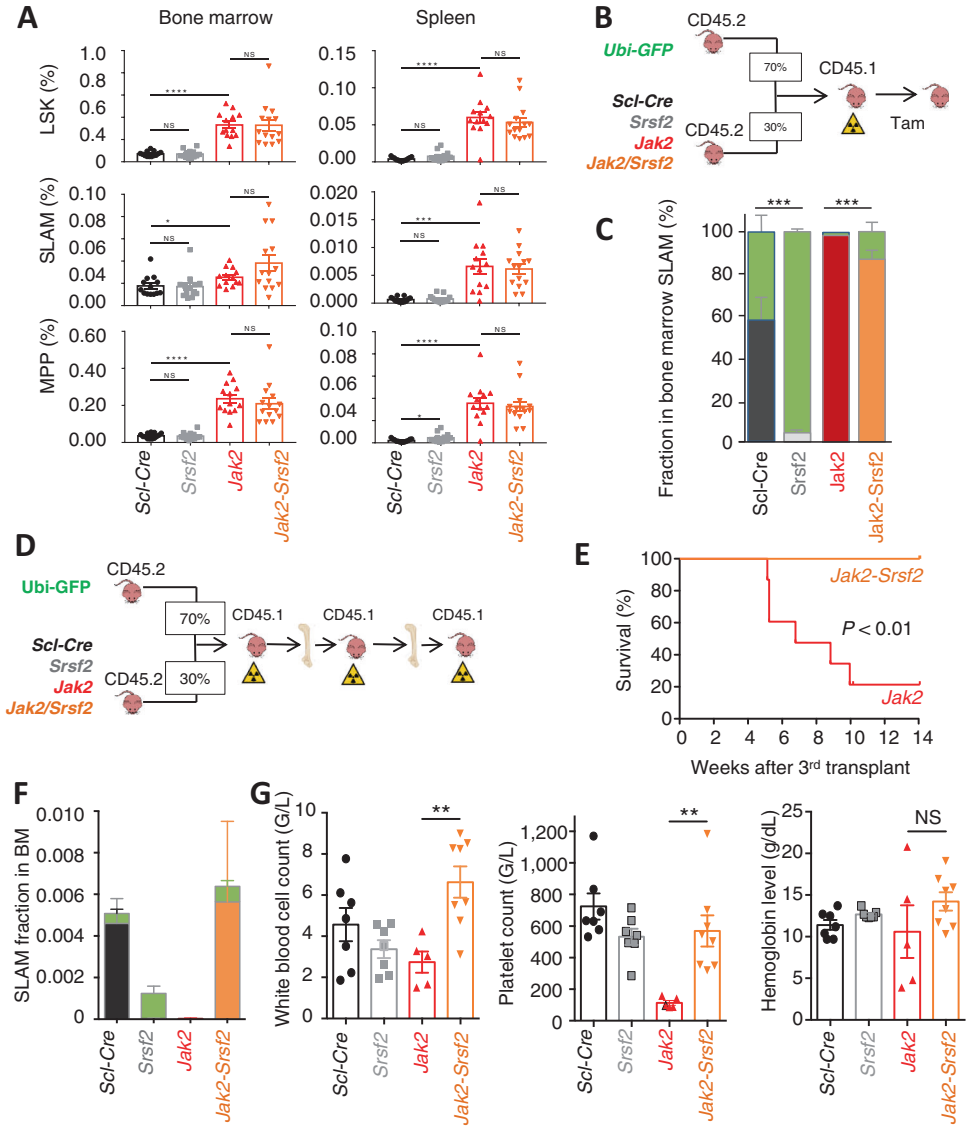

Fig. 2 *Srsf2*^{P95H} co-mutation reduces *Jak2*^{V617F} cell competitiveness. A Bone marrow cells were engrafted as in Fig. 1A; flow cytometry measurement of LSK (Lin$^-$,Sca1$^+$, cKit$^+$), SLAM (LSK, CD48$^-$, CD150$^+$) and MPP (LSK, CD48$^+$, CD150$^-$) fractions in bone marrow and spleen collected from indicated mouse strains (black *Scl-Cre*, gray *Srsf2*^{P95H}, red *Jak2*^{V617F}, orange *Jak2*^{V617F}/*Srsf2*^{P95H}), 16–24 weeks after tamoxifen gavage; pooled analysis of 2 experiments: *Scl-Cre* ($n = 13$), *Srsf2*^{P95H} ($n = 13$), *Jak2*^{V617F} ($n = 13$), *Jak2*^{V617F}/*Srsf2*^{P95H} ($n = 14$); **B** A mixture of whole bone marrow cells collected from one of the indicated CD45.2 mouse strains (0.9×10^6; 30%) and CD45.2 *Ubi*-GFP transgenic mice (2.1×10^6, 70%) were engrafted into lethally irradiated CD45.1 recipients, 5 weeks before tamoxifen gavage (10 mg/day, 2 days); **C** Flow cytometry measurement of bone marrow GFP$^+$ (in green) and GFP$^-$ (colors indicate strains as in panel A) CD45.2$^+$ SLAM repartition in the bone marrow, 24 weeks after tamoxifen gavage; $n = 7$ mice per group, mean ± SEM; **D** Following a first transplantation as in (**B**), bone marrow cells (3×10^6) were serially transplanted into CD45.1 mice (second transplantation, 24 weeks after tamoxifen gavage; third transplantation 16 weeks after transplantation); **E** Overall survival of mice after the third transplantation with *Jak2*^{V617F} (in red) and *Jak2*^{V617F}/*Srsf2*^{P95H} (in orange) containing bone marrow cells. *Jak2*^{V617F} ($n = 8$), *Jak2*^{V617F}/*Srsf2*^{P95H} ($n = 8$); **F** Flow cytometry measurement of bone marrow GFP$^+$ (shown in green) and GFP$^-$, CD45.2$^+$ SLAM fraction among bone marrow cells in sacrificed animals; **G** Peripheral blood white blood cell count, platelet count and hemoglobin level following the third transplantation, 16 weeks after transplantation (except *Jak2*, last blood cell analysis before death); *Scl-Cre* ($n = 7$), *Srsf2*^{P95H} ($n = 7$), *Jak2*^{V617F} ($n = 5$), *Jak2*^{V617F} *Srsf2*^{P95H} ($n = 8$); mean ± SEM; All panel, unpaired t-test. *$P < 0.05$; **$P < 0.01$; ***$P < 0.001$; ****$P < 0.0001$. NS not significant.

We detected 666 differential splicing events in *Srsf2*^{P95H} cells. We also identified 587 differential splicing events in *Jak2*^{V617F} cells, which may reflect the ability of mutant JAK2 to phosphorylate proteins involved in mRNA processing [27]. The highest number ($n = 1241$) was observed in double-mutant *Jak2*^{V617F}/*Srsf2*^{P95H} megakaryocytes. One hundred thirty four events (7.7% of total) were common to the three genetically modified cell populations (Fig. 5B).

Given the importance of the JAK/STAT pathway activation in MFs, we focused on differential splicing events that affect genes of this pathway. Of the 147 genes listed in KEGG_JAK_STAT_SIGNALING_PATHWAY, 16 showed abnormal splicing events, with only one common to the three cell types (*il15ra* gene). One of the two abnormally spliced genes common to *Srsf2*^{P95H} and *Jak2*^{V617F}/*Srsf2*^{P95H} cells, but not detected in *Jak2*^{V617F} cells, was *Jak2* (Fig. 5C, Supplementary Table 1).

In *Srsf2*^{P95H} expressing cells, an abnormal skipping of *Jak2* exon 14 (*Jak2*$^{\Delta ex14}$), which encodes the pseudokinase domain including Valine 617, results in a frameshift (Fig. 5D). Using an isoform-specific RT-qPCR, *Jak2*$^{\Delta ex14}$ was detected in LSK (Lin$^-$,Sca$^+$,Kit$^+$)

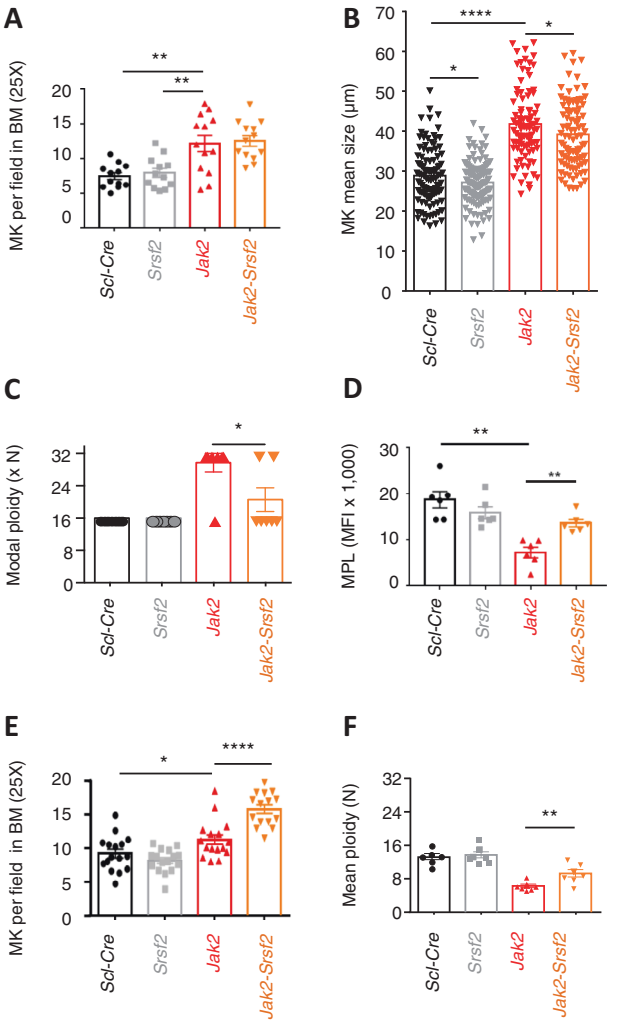

Fig. 3 Impact of *Srsf2*^{P95H} on *Jak2*^{V617F}-induced megakaryocyte phenotypic modifications. A–D Analysis of bone marrow collected 8 weeks post-tamoxifen; **A** Number of vWF-stained megakaryocytes per field of bone marrow sections in indicated mice (mean ± SEM); **B** Mean size of megakaryocytes according to the genotype (mean ± SEM); **C** Modal ploidy measured in megakaryocytes (mean ± SEM). **D** Expression of the thrombopoietin receptor MPL on megakaryocytes (MFI, mean fluorescence index); **E**, **F** Analysis of bone marrow collected 16–24 weeks post-tamoxifen; **E** Number of vWF-stained megakaryocytes per field of bone marrow sections in indicated mice (mean ± SEM); **F** Mean ploidy measured in megakaryocytes (mean ± SEM). All figures were analyzed using unpaired t-test., $*P < 0.05$; $**P < 0.01$; $***P < 0.001$; ns non-significant.

cells, erythroid cells (CD71^{+}, Ter119^{+}) and megakaryocytes sorted from the BM of *Srsf2*^{P95H} and *Jak2*^{V617F}/*Srsf2*^{P95H} animals (Fig. 5D, Supplementary Fig. 5A, B). This alternatively spliced *Jak2* was no more detected in megakaryocytes when these cells were generated by ex vivo differentiation of LSK in the presence of TPO, suggesting a counter-selection of cells expressing *Jak2*$^{\Delta ex14}$ isoform in these culture conditions (Fig. 5D). Importantly, a *JAK2*$^{\Delta ex14}$ isoform could be detected also in peripheral blood granulocytes collected from two *JAK2*^{V617F} MF patients with a co-existing *SRSF2*^{P95} mutation, while not being detected in the cells of two healthy donors and three JAK2^{V617F} MF patients without *SRSF2* mutation (Fig. 5E).

The presence of a *Jak2*$^{\Delta ex14}$ isoform correlated with a decrease in the level of phosphorylated STAT5 measured by flow cytometry in sorted LSK cells (Fig. 5F and Supplementary 5C). When transfected in γ−2A cells, *Jak2*$^{\Delta ex14}$ isoform was translated into a shortened protein at the expected 66 kDa molecular weight (Fig. 5G). Using a dual luciferase assay in γ−2A cells expressing the thrombopoietin receptor MPL, we observed that the shortened protein encoded by JAK2$^{\Delta ex14}$ (Fig. 5G) did not transduce a P-STAT5 signal in response to thrombopoietin (Fig. 5G, H). When JAK2^{V617F} was co-expressed with JAK2$^{\Delta ex14}$ at various ratio in γ−2A cells, JAK2$^{\Delta ex14}$ isoform behave like the empty vector, in the absence or presence of thrombopoietin (Fig. 5I). These results suggested a loss of function of JAK2$^{\Delta ex14}$ that may explain the weaker phenotype observed when the Srsf2^{P95H} mutation is combined with Jak2^{V617F} through a quantitative decrease in the functional JAK2^{V617F} (Fig. 5D and Supplementary 5A).

Srsf2^{P95H} down-regulates romiplostim-induced MF

Since Srsf2^{P95H} induces the abnormal skipping of JAK2 exon 14, generating a truncated and inactive protein, we wanted to further validate Srsf2^{P95} mutation effect on JAK/STAT signaling. Therefore, we used a previously described mouse model of MF induced by subcutaneous administration of high dose romiplostim, a thrombopoietin receptor agonist that generates MPL-mediated hypersignalling. Animals were engrafted with either *Scl-Cre* or *Srsf2*^{P95H} bone marrow cells. Three weeks after tamoxifen gavage, they received three weekly administration of high dose (1 mg/kg/day) romiplostim (Fig. 6A). This treatment induced a rapid increase in the peripheral blood platelet count, which was significantly less important in *Srsf2*^{P95H} engrafted animals (Fig. 6B). All the *Scl-Cre* engrafted animals developed a MF, which was reduced in *Srsf2*^{P95H} engrafted animals (Fig. 6C, D), an effect that was also observed in the spleen (Fig. 6E). Together, these results validated that the *Srsf2*^{P95H} genotype negatively interfered with MF induction upon JAK/STAT hypersignaling, either induced by Jak2 mutation or MPL stimulation.

DISCUSSION

The present study demonstrates that *Srsf2*^{P95H} delays myelofibrosis when associated with *Jak2*^{V617F} in mouse hematopoietic cells. *Srsf2*^{P95H} promotes *JAK2* exon 14 skipping in mouse and human hematopoietic cells. This event generates a shortened, non-functional protein that may contribute to decreasing JAK/STAT signaling. These results contrast with the cooperative effect of deletion of *Ezh2*, *Asxl1* and *Dnmt3a* with *Jak2*^{V617F} to exacerbate MF in mice [10–14].

Several knock-in murine models of *Srsf2* mutation have been generated [21, 28, 29]. They recapitulated human diseases to varying extents, with a common engraftment defect of mutated cells contrasting with the positive selection of *SRSF2*-mutant cells in humans [30]. However, this poor competitive engraftment of *Srsf2*^{P95H} mouse BM cells diseappears when competitor cells and microenviromnement are matched for age [29, 30]. Since the clonal selection of *SRSF2*^{P95H} hematopoietic cells is also associated with aging in humans [31–33], cell and tissue aging may be required for the mutated splicing factor to accelerate clonal growth [33] and generate a full-blown disease phenotype. Alternatively, additional mutational events in the context of *JAK2* and *SRSF2* co-mutation could account for the severe outcome associated with this molecular background [17].

The abnormal maturation of megakaryocytes is a characteristic feature of *Jak2*^{V617F} expression. These abnormal megakaryocytes are critical drivers of BM fibrosis, i.e., they reprogram hematopoiesis-supporting cells to fibrosis-driving cells [34]. Accordingly, targeting megakaryocytes ameliorates MF in preclinical models and early phase clinical studies [35–37]. Mouse models of MPNs expressing *Jak2*^{V617F} were shown to demonstrate an increased proportion of megakaryocyte-biased CD41^{high} HSPCs [38], and recent investigation at the single cell level validated the aberrant differentiation of HSPCs with an expansion of megakaryocyte progenitors exhibiting an abnormal gene signature

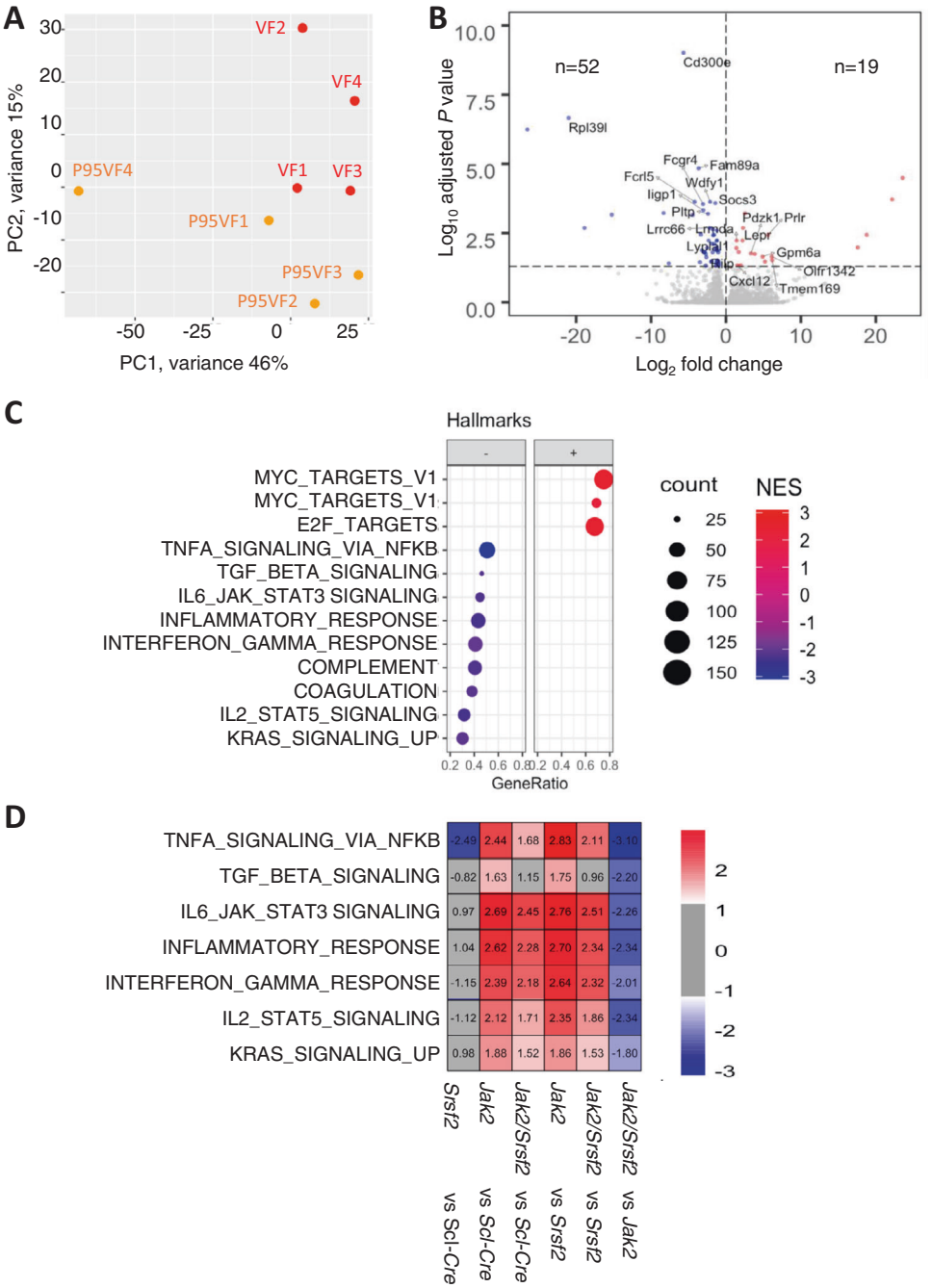

Fig. 4 ***Srsf2*^{P95H} co-mutation with *Jak2*^{V617F} down-regulates genes involved in signaling pathways.** Megakaryocytes sorted from mouse bone marrow engrafted as in Fig. 1A and sacrificed 8 weeks post tamoxifen were analyzed by bulk RNA sequencing (metadata in Supplementary Table 3). **A** Principal component analysis (PCA) of *Jak2*^{V617F} (red, VF) and *Jak2*^{V617F}/*Srsf2*^{P95H} (orange, P95VF) mouse megakaryocytes; **B** Volcanoplot of differentially expressed genes (DEGs) between *Jak2*^{V617F} and *Jak2*^{V617F}/*Srsf2*^{P95H} megakaryocytes, numbers indicate down-regulated ($n = 52$) and up-regulated ($n = 19$) genes in *Jak2*^{V617F}/*Srsf2*^{P95H}cells; **C** Hallmark pathway analysis of the comparison between *Jak2*^{V617F} and *Jak2*^{V617F}/*Srsf2*^{P95H} megakaryocytes; **D** Enrichment score of signaling pathways among mouse models (up-regulated in red, down-regulated in blue, not significantly modified in gray).

associated with fibrosis [39]. At the molecular level, aberrant megakaryocyte number, differentiation, location and function were associated with the decreased expression of GATA1 protein [40], the overexpression of the anti-apoptotic protein Bcl-X_L [41, 42], and irregular production of fibrogenic cytokines including TGFβ1 [43, 44]. In the mouse model described here, *Srsf2*^{P95H} does not restore a wild-type megakaryocyte phenotype but attenuates the phenotypic alterations induced by *Jak2*^{V617F} and reduces TGFβ1 level.

STAT3 and STAT5 are commonly activated in human MPN, downstream of MPL and JAK2 [45–47]. Some differences can be detected in signaling output between genotype subtypes [48]. Transgenic expression of a dominant negative STAT3 mutant delays platelet recovery after myelosuppression [49] but, in the context of *Jak2*^{V617F}, *Stat3* deletion enhances thrombocytosis and shortens survival of mutated animals [50]. STAT5 plays a central role in mouse models of *Jak2*^{V617F}-induced MPN [51, 52], animals deficient for STAT5 are thrombocytopenic [53], and STAT5 target

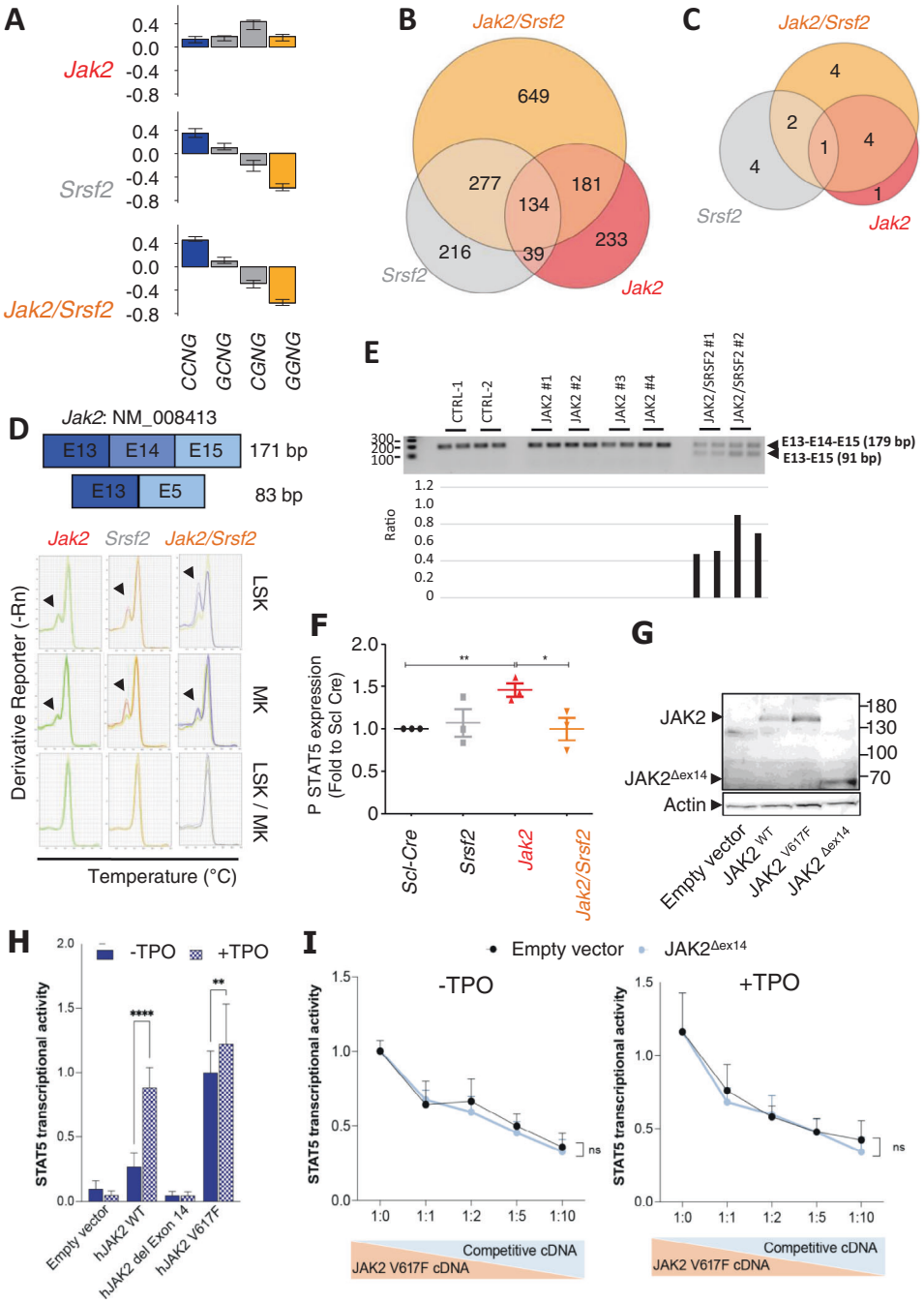

Fig. 5 ***Srsf2*^{P95H} promotes Jak2 exon 14 skipping.** **A** Relative enrichment of all four SSNG variants, where S represents C or G, in cassette exons that are differentially spliced in BM megakaryocytes sorted from *Jak2*^{V617F}, *Srsf2*^{P95H} and *Jak2*^{V617F} / *Srsf2*^{P95H} animals compared to *Scl-Cre* megakaryocytes ($n = 4$ per group). **B** Venn diagram indicating the number of splicing events (False Discovery Rate (FDR) < 0.05), in mutated compared to *Scl-Cre* megakaryocytes. **C** Venn diagram of differential splicing events (FDR < 0.05) among the 147 genes listed in KEGG_JAK_STAT_SIGNALING_PATHWAY in mutated compared to *Scl-Cre* megakaryocytes. **D** RT-PCR analysis of alternatively spliced isoforms of mouse *Jak2*. Upper panel, scheme of the detected 171 bp (exon 14 included) and 83 bp (exon 14 excluded) *Jak2* cDNA fragments; RT-qPCR dissociation curve showing the 2 amplicons (higher peak, 171 bp, exon 14 included; lower peak, 83 bp, exon 14 excluded/arrows). Upper line: sorted megakaryocytes; middle line: sorted BM LSK; lower line, megakaryocytes generated ex vivo by culturing LSK with TPO. **E** RT-PCR analysis of alternatively spliced isoforms of human *JAK2*: gel migration of RT-qPCR products in granulocytes of 2 healthy donors, 4 patients with *JAK2* but no *SRSF2* mutation and 2 patients with both *SRSF2* and *JAK2* mutations. Lower panel: Image J quantification. **F** Flow cytometry analysis of P-STAT5 in sorted BM LSK cells from indicated mice (3 per group). **G** Immunoblot detection of JAK2 full length with or without V617F mutation (~130 kDa) and JAK2$^{\Delta Ex14}$ (~68 kDa) expressed in γ-2A cells. **H** STAT5 transcriptional activity measured in γ2a cells transduced with TPO receptor and indicated JAK2 constructs without (dotted blue) and with (full blue) stimulation with TPO (10 ng/ml). Mean ± SD of 3 independent experiments performed in triplicates. **I** STAT5 trancriptional activity measured in γ2a cells transduced with various ratio of JAK2 V617F and JAK2$^{\Delta Ex14}$ or an empty vector, without (left) or with (right) Tpo stimulation (10 ng/ml). Mean ± SD of 3 independent experiments performed in triplicates. **G**, **H** Statistics: two-ways ANOVA followed by SIDAK multiple comparison test. ****$p < 0.0001$, **$p < 0.01$, ns non-significant.

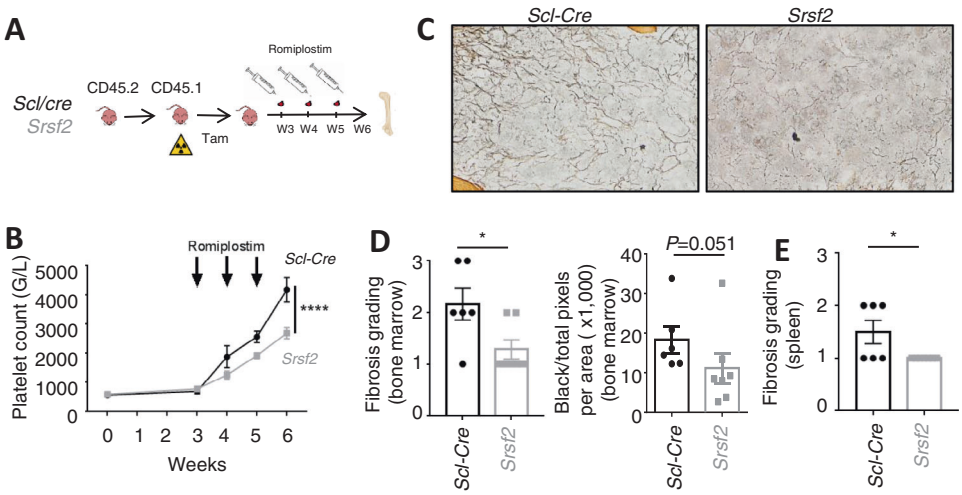

Fig. 6 *Srsf2*^{P95H} delays romiplositim-induced myelofibrosis. A Mice engrafted with 3×10^6 *Scl-Cre* or *Srsf2*^{P95H} bone marrow cells were treated with tamoxifen as in Fig. 1A. Three weeks later, they received subcutaneous injections of romiplostim (1 mg/kg) every week for 3 weeks and peripheral blood was collected for blood cell count. Animals were sacrificed at day 21. **B** Evolution of platelet count in *Scl-Cre* or *Srsf2*^{P95H} transplanted animals upon romiplostim treatment; **C** Bone marrow section after Gordon and Sweet's staining of *Scl-Cre* or *Srsf2*^{P95H} transplanted animals at day 21; **D** Myelofibrosis in romiplostim-treated, *Scl-Cre* or *Srsf2*^{P95H} transplanted mice at day 21, evaluated by either grading (left panel) or image J quantification of reticulin fibers (right panel); **E** Spleen fibrosis was evaluated by grading in the same animals. Kruskal-Wallis test, *$P < 0.05$; **$P < 0.01$; NS non-significant.

genes are up-regulated in *Jak2*^{V617F} megakaryocytes [54]. The decreased activation of STAT5 detected in LSK cells when *Srsf2*^{P95H} is co-expressed with *Jak2*^{V617F} may therefore contribute to the delayed phenotype observed in double-mutated animals.

Modulation of JAK/STAT pathway activity by alternative splicing of constitutive genes was described in Hodgkin lymphoma cells in which an alternative isoform of protein-tyrosine phosphatase 1B enhances JAK/STAT activity [55]. Mutation of the Proline 95 residue in SRSF2, which alters its RNA binding specificity, generates a number of mis-spliced transcripts in hematopoietic cells [20, 28–30, 56–58]. Here, we identify the ability of *SRSF2*^{P95H} to promote *JAK2* exon 14 skipping. This exon encodes the JAK-homology 2 (JH2) domain, a pseudokinase domain in which the valine residue 617 is located. This domain both suppresses basal JAK2 activity in the absence of cytokine stimulation and is required for induction of maximal JAK2 activation, i.e., to render JAK2 responsive to cytokine stimulation with increased activity [59, 60]. Deletion of *JAK2* exon 14 was already detected as a minor splice variant of *JAK2* (~12% of JAK2 mRNA) in the granulocytes of patients with MF, without analysis of *SRSF2* sequence [61, 62]. *JAK2* exon 14 skipping induced by *Srsf2*^{P95H} generates a frameshift with the synthesis of a truncated protein without kinase domain and thus unable to induce downstream signaling. This isoform does not generate a dominant negative protein, thus may decrease JAK/STAT signaling by decreasing the amount of functional full-length JAK2 protein, which, on the long term, may contribute to delay myelofibrosis development.

The decreased expression of the thrombopoietin receptor MPL at the surface of megakaryocytes and platelets is an established feature of MF [25, 63]. There is evidence that this decrease is related both to the loss of the chaperone activity of JAK2 by JAK2^{V617F} and to increased MPL activation and internalization with reduced recycling. Our finding that *Srsf2*^{P95H} partially restores the expression of MPL at the surface of megakaryocytes further argues for an altered activity of Jak2^{V617F} protein is mouse cells. The delayed induction of thrombocytosis and MF by romiplostim [64] observed in mice expressing *Srsf2*^{P95H} in a *Jak2* wild-type background, further supports a negative impact of *Srsf2*^{P95H} on megakaryocyte signaling, downstream of MPL, which may involve *Jak2* exon 14 skipping.

Taken together, we have depicted an unexpected interplay between *Jak2*^{V617F} and *Srsf2*^{P95H} when co-expressed in hematopoietic cells. *Jak2* exon 14 skipping promoted by mutated SRSF2, which is detected also in patients with a *Jak2*^{V617F}/*Srsf2*^{P95H} myelofibrosis, generates a truncated, inactive JAK2. Additional events, which could be related with ageing of HSCPs and bone marrow niche cells, must overcome the decrease in JAK/STAT signaling in patients with *Jak2*^{V617F}/*Srsf2*^{P95H} co-mutation to promote clonal expansion. Regardless of these mechanisms, our results suggest that understanding the molecular mechanisms involved in *JAK2* alternative splicing could potentially drive innovative strategies to reduce JAK/STAT signaling in pathological conditions.

DATA AVAILABILITY

Data are available in BioStudies under accession number: E-MTAB-11960.

REFERENCES

1. Vainchenker W, Kralovics R. Genetic basis and molecular pathophysiology of classical myeloproliferative neoplasms. Blood. 2017;129:667–79.
2. Gangat N, Tefferi A. Myelofibrosis biology and contemporary management. Br J Haematol. 2020;191:152–70.
3. Decker M, Martinez-Morentin L, Wang G, Lee Y, Liu Q, Leslie J, et al. Leptin-receptor-expressing bone marrow stromal cells are myofibroblasts in primary myelofibrosis. Nat Cell Biol. 2017;19:677–88.
4. Schneider RK, Mullally A, Dugourd A, Peisker F, Hoogenboezem R, Van Strien PMH, et al. Gli1$^+$ Mesenchymal Stromal Cells Are a Key Driver of Bone Marrow Fibrosis and an Important Cellular Therapeutic Target. Cell Stem Cell. 2018;23:308–9.
5. Leimkühler NB, Gleitz HFE, Ronghui L, Snoeren IAM, Fuchs SNR, Nagai JS, et al. Heterogeneous bone-marrow stromal progenitors drive myelofibrosis via a druggable alarmin axis. Cell Stem Cell. 2021;28:637–52.e8.
6. Martyré M, Romquin N, Le Bousse-Kerdiles MC, Chevillard S, Benyahia B, Dupriez B, et al. Transforming growth factor-beta and megakaryocytes in the pathogenesis of idiopathic myelofibrosis. Br J Haematol. 1994;88:9–16.
7. Vannucchi AM, Bianchi L, Paoletti F, Pancrazzi A, Torre E, Nishikawa M, et al. A pathobiologic pathway linking thrombopoietin, GATA-1, and TGF-beta1 in the development of myelofibrosis. Blood. 2005;105:3493–501.
8. Frangogiannis N. Transforming growth factor-β in tissue fibrosis. J Exp Med. 2020;217:e20190103.

9. Grinfeld J, Nangalia J, Baxter EJ, Wedge DC, Angelopoulos N, Cantrill R, et al. Classification and Personalized Prognosis in Myeloproliferative Neoplasms. N Engl J Med. 2018;379:1416–30.
10. Shimizu T, Kubovcakova L, Nienhold R, Zmajkovic J, Meyer SC, Hao-Shen H, et al. Loss of Ezh2 synergizes with JAK2-V617F in initiating myeloproliferative neoplasms and promoting myelofibrosis. J Exp Med. 2016;213:1479–96.
11. Yang Y, Akada H, Nath D, Hutchison RE, Mohi G. Loss of Ezh2 cooperates with Jak2V617F in the development of myelofibrosis in a mouse model of myeloproliferative neoplasm. Blood. 2016;127:3410–23.
12. Sashida G, Wang C, Tomioka T, Oshima M, Aoyama K, Kanai A, et al. The loss of Ezh2 drives the pathogenesis of myelofibrosis and sensitizes tumor-initiating cells to bromodomain inhibition. J Exp Med. 2016;213:1459–77.
13. Guo Y, Zhou Y, Yamatomo S, Yang H, Zhang P, Chen S, et al. ASXL1 alteration cooperates with JAK2V617F to accelerate myelofibrosis. Leukemia. 2019;33:1287–91.
14. Jacquelin S, Straube J, Cooper L, Vu T, Song A, Bywater M, et al. Jak2V617F and Dnmt3a loss cooperate to induce myelofibrosis through activated enhancer-driven inflammation. Blood. 2018;132:2707–21.
15. Yoshida K, Sanada M, Shiraishi Y, Nowak D, Nagata Y, Yamamoto R, et al. Frequent pathway mutations of splicing machinery in myelodysplasia. Nature. 2011;478:64–9.
16. Todisco G, Creignou M, Gallì A, Guglielmelli P, Rumi E, Roncador M, et al. Co-mutation pattern, clonal hierarchy, and clone size concur to determine disease phenotype of SRSF2^{P95}-mutated neoplasms. Leukemia. 2021;35:2371–81.
17. Lasho T, Jimma T, Finke CM, Patnaik M, Hanson CA, Ketterling RP, et al. SRSF2 mutations in primary myelofibrosis: significant clustering with IDH mutations and independent association with inferior overall and leukemia-free survival. Blood. 2012;120:4168–71.
18. Guglielmelli P, Pacilli A, Rotunno G, Rumi E, Rosti V, Delaini F, et al. Presentation and outcome of patients with 2016 WHO diagnosis of prefibrotic and overt primary myelofibrosis. Blood. 2017;129:3227–36.
19. Guglielmelli P, Biamonte F, Rotunno G, Artusi V, Artuso L, Bernardis I, et al. Impact of mutational status on outcomes in myelofibrosis patients treated with ruxolitinib in the COMFORT-II study. Blood. 2014;123:2157–60.
20. Hasan S, Lacout C, Marty C, Cuingnet M, Solary E, Vainchenker W, et al. JAK2V617F expression in mice amplifies early hematopoietic cells and gives them a competitive advantage that is hampered by IFNα. Blood. 2013;122:1464–77.
21. Kim E, Ilagan JO, Liang Y, Daubner GM, Lee SC, Ramakrishnan A, et al. SRSF2 Mutations Contribute to Myelodysplasia by Mutant-Specific Effects on Exon Recognition. Cancer Cell. 2015;27:617–30.
22. Göthert JR, Gustin SE, Hall MA, Green AR, Göttgens B, Izon DJ, et al. In vivo fate-tracing studies using the Scl stem cell enhancer: embryonic hematopoietic stem cells significantly contribute to adult hematopoiesis. Blood. 2005;105:2724–32.
23. Benlabiod C, Cacemiro MDC, Nédélec A, Edmond V, Muller D, Rameau P, et al. Calreticulin del52 and ins5 knock-in mice recapitulate different myeloproliferative phenotypes observed in patients with MPN. Nat Commun. 2020;11:4886.
24. Staerk J, Defour JP, Pecquet C, Leroy E, Antoine-Poirel H, Brett I, et al. Orientation-specific signalling by thrombopoietin receptor dimers. EMBO J. 2011;30:4398–413.
25. Pecquet C, Diaconu CC, Staerk J, Girardot M, Marty C, Royer Y, et al. Thrombopoietin receptor down-modulation by JAK2 V617F: restoration of receptor levels by inhibitors of pathologic JAK2 signaling and of proteasomes. Blood. 2012;119:4625–35.
26. Daubner GM, Clery A, Jayne S, Stevenin J, Allain FHT. A syn-anti conformational difference allows SRSF2 to recognize guanines and cytosines equally well. EMBO J. 2012;31:162–74.
27. Jayavelu AK, Schnöder TM, Perner F, Herzog C, Meiler A, Krishnamoorthy G, et al. Splicing factor YBX1 mediates persistence of JAK2-mutated neoplasms. Nature. 2020;588:157–63.
28. Kon A, Yamazaki S, Nannya Y, Kataoka K, Ota Y, Nakagawa MM, et al. Physiological Srsf2 P95H expression causes impaired hematopoietic stem cell functions and aberrant RNA splicing in mice. Blood. 2018;131:621–35.
29. Smeets MF, Tan SY, Xu JJ, Anande G, Unnikrishnan A, Chalk AM, et al. Srsf2(P95H) initiates myeloid bias and myelodysplastic/ myeloproliferative syndrome from hemopoietic stem cells. Blood. 2018;132:608–21.
30. Xu JJ, Smeets MF, Tan SY, Wall M, Purton LE, Walkley CR. Modeling human RNA spliceosome mutations in the mouse: not all mice were created equal. Exp Hematol. 2019;70:10–23.
31. McKerrell T, Park N, Moreno T, Grove CS, Ponstingl H, Stephens J, et al. Leukemia-associated somatic mutations drive distinct patterns of age-related clonal hemopoiesis. Cell Rep. 2015;10:1239–45.
32. Bartels S, Faisal M, Büsche G, Schlue J, Hasemeier B, Schipper E, et al. Mutations associated with age-related clonal hematopoiesis in PMF patients with rapid progression to myelofibrosis. Leukemia. 2020;34:1364–72.
33. Fabre MA, de Almeida JG, Fiorillo E, Mitchell E, Damaskou A, Rak J, et al. The longitudinal dynamics and natural history of clonal haematopoiesis. Nature. 2022;606:335–42.
34. Kramann R, Schneider RK. The identification of fibrosis-driving myofibroblast precursors reveals new therapeutic avenues in myelofibrosis. Blood. 2018;131:2111–9.
35. Wen QJ, Yang Q, Goldenson B, Malinge S, Lasho T, Schneider RK, et al. Targeting megakaryocytic-induced fibrosis in myeloproliferative neoplasms by AURKA inhibition. Nat Med. 2015;21:1473–80.
36. Eliades A, Papadantonakis N, Bhupatiraju A, Burridge KA, Johnston-Cox HA, Migliaccio AR, et al. Control of megakaryocyte expansion and bone marrow fibrosis by lysyl oxidase. J Biol Chem. 2011;286:27630–8.
37. Gangat N, Marinaccio C, Swords R, Watts JM, Gurbuxani S, Rademaker A, et al. Aurora Kinase A Inhibition Provides Clinical Benefit, Normalizes Megakaryocytes, and Reduces Bone Marrow Fibrosis in Patients with Myelofibrosis: A Phase I Trial. Clin Cancer Res. 2019;25:4898–906.
38. Rao TN, Hansen N, Stetka J, Luque Paz D, Kalmer M, Hilfiker J, et al. JAK2-V617F and interferon-α induce megakaryocyte-biased stem cells characterized by decreased long-term functionality. Blood. 2021;137:2139–51.
39. Psaila B, Wang G, Rodriguez-Meira A, Li R, Heuston EF, Murphy L, et al. Single-Cell Analyses Reveal Megakaryocyte-Biased Hematopoiesis in Myelofibrosis and Identify Mutant Clone-Specific Targets. Mol Cell. 2020;78:477–92.e8.
40. Gilles L, Arslan AD, Marinaccio C, Wen QJ, Arya P, McNulty M, et al. Down-regulation of GATA1 drives impaired hematopoiesis in primary myelofibrosis. J Clin Investig. 2017;127:1316–20.
41. Ciurea SO, Merchant D, Mahmud N, Ishii T, Zhao Y, Hu W, et al. Pivotal contributions of megakaryocytes to the biology of idiopathic myelofibrosis. Blood. 2007;110:986–93.
42. Masselli E, Carubbi C, Gobbi G, Mirandola P, Galli D, Martini S, et al. Protein kinase Ce inhibition restores megakaryocytic differentiation of hematopoietic progenitors from primary myelofibrosis patients. Leukemia. 2015;29:2192–201.
43. Zahr AA, Salama ME, Carreau N, Tremblay D, Verstovsek S, Mesa R, et al. Bone marrow fibrosis in myelofibrosis: pathogenesis, prognosis and targeted strategies. Haematologica. 2016;101:660–71.
44. Varricchio L, Iancu-Rubin C, Upadhyaya B, Zingariello M, Martelli F, Verachi P, et al. TGF-β1 protein trap AVID200 beneficially affects hematopoiesis and bone marrow fibrosis in myelofibrosis. JCI Insight. 2021;6:e145651.
45. Kleppe M, Kwak M, Koppikar P, Riester M, Keller M, Bastian L, et al. JAK-STAT pathway activation in malignant and nonmalignant cells contributes to MPN pathogenesis and therapeutic response. Cancer Discov. 2015;5:316–31.
46. Woods B, Chen W, Chiu S, Marinaccio C, Fu C, Gu L, et al. Activation of JAK/STAT Signaling in Megakaryocytes Sustains Myeloproliferation In Vivo. Clin Cancer Res. 2019;25:5901–12.
47. Rampal R, Al-Shahrour F, Abdel-Wahab O, Patel JP, Brunel JP, Mermel CH, et al. Integrated genomic analysis illustrates the central role of JAK-STAT pathway activation in myeloproliferative neoplasm pathogenesis. Blood. 2014;123:e123–33.
48. Sakr H, Schneider Clark, Murugesan K, Bodo G, His J, Cook ED, et al. pSTAT3/pSTAT5 Signaling Patterns in Molecularly Defined Subsets of Myeloproliferative Neoplasms. Appl Immunohistochem Mol Morphol. 2018;26:147–52.
49. Kirito K, Osawa M, Morita H, Shimizu R, Yamamoto M, Oda A, et al. A functional role of Stat3 in in vivo megakaryopoiesis. Blood. 2002;99:3220–7.
50. Grisouard J, Shimizu T, Duek A, Kubovcakova L, Hao-Shen H, Dirnhofer S, et al. Deletion of Stat3 in hematopoietic cells enhances thrombocytosis and shortens survival in a JAK2-V617F mouse model of MPN. Blood. 2015;125:2131–40.
51. Yan D, Hutchison RE, Mohi G. Critical requirement for Stat5 in a mouse model of polycythemia vera. Blood. 2012;119:3539–49.
52. Walz C, Ahmed W, Lazarides K, Betancur M, Patel N, Hennighausen L, et al. Essential role for Stat5a/b in myeloproliferative neoplasms induced by BCR-ABL1 and JAK2(V617F) in mice. Blood. 2012;119:3550–60.
53. Snow JW, Abraham N, Ma MC, Abbey NW, Herndier B, Goldsmith MA. STAT5 promotes multilineage hematolymphoid development in vivo through effects on early hematopoietic progenitor cells. Blood. 2002;99:95–101.
54. Lau WW, Hannah R, Green AR, Göttgens B. The JAK-STAT signaling pathway is differentially activated in CALR-positive compared with JAK2V617F-positive ET patients. Blood. 2015;125:1679–81.
55. Zahn M, Marienfeld R, Melzner I, Heinrich J, Renner B, Wegener S, et al. A novel PTPN1 splice variant upregulates JAK/STAT activity in classical Hodgkin lymphoma cells. Blood. 2017;129:1480–90.
56. Zhang J, Lieu YK, Ali AM, Penson A, Reggio KS, Rabadan R, et al. Disease-associated mutation in SRSF2 misregulates splicing by altering RNA-binding affinities. Proc Natl Acad Sci USA. 2015;112:E4726–34.
57. Lee SC, North K, Kim E, Jang E, Obeng E, Lu SX, et al. Synthetic Lethal and Convergent Biological Effects of Cancer-Associated Spliceosomal Gene Mutations. Cancer Cell. 2018;34:225–41.e8.

58. Yoshimi A, Lin KT, Wiseman DH, Rahman MA, Pastore A, Wang B, et al. Coordinated alterations in RNA splicing and epigenetic regulation drive leukaemogenesis. Nature. 2019;574:273–7.
59. Saharinen P, Silvennoinen O. The pseudokinase domain is required for suppression of basal activity of Jak2 and Jak3 tyrosine kinases and for cytokine-inducible activation of signal transduction. J Biol Chem. 2002;277:47954–63.
60. Saharinen P, Vihinen M, Silvennoinen O. Autoinhibition of Jak2 tyrosine kinase is dependent on specific regions in its pseudokinase domain. Mol Biol Cell. 2003;14:1448–59.
61. Ma W, Kantarjian H, Zhang X, Wang X, Zhang Z, Yeh CH, et al. JAK2 exon 14 deletion in patients with chronic myeloproliferative neoplasms. PLoS ONE. 2010;5:e12165.
62. Catarsi P, Rosti V, Morreale G, Poletto V, Villani L, Bertorelli R, et al. JAK2 exon 14 skipping in patients with primary myelofibrosis: a minor splice variant modulated by the JAK2-V617F allele burden. PLoS ONE. 2015;10:e0116636.
63. Sangkhae V, Etheridge SL, Kaushansky K, Hitchcock IS. The thrombopoietin receptor, MPL, is critical for development of a JAK2V617F-induced myeloproliferative neoplasm. Blood. 2014;124:3956–63.
64. Kuter DJ, Mufti GJ, Bain BJ, Hasserjian RP, Davis W, Rutstein M. Evaluation of bone marrow reticulin formation in chronic immune thrombocytopenia patients treated with romiplostim. Blood. 2009;114:3748–56.

ACKNOWLEDGEMENTS

We thank the engineers and technicians of Gustave Roussy research facilities, including Laure Touchard, Mirile Ganga, Olivia Bawa, and Hélène Rocheteau, for valuable technical support, Richard Dyunga and Inge Snoeren (Erasmus University Rotterdam) for animal genotyping and nucleic acid extraction, respectively. ES group is supported by grants from the Institut National du Cancer (INCa) and Fondation ARC. The team is labeled by the Ligue Nationale Contre le Cancer (FP). CW received an MD/PhD track grant from the Philantropia Foundation. Funding to SNC is acknowledged from Ludwig Institute for Cancer Research, Fondation contre le cancer, Salus Sanguinis and Fondation "Les avions de Sébastien", projets Action de recherché concertée (ARC) 16/21-073, Projet de recherche FNRS n°T.0043.21 and WelBio F 44/8/5—MCF/UIG—10955. IP, VW, CM and JLV received support from the MPN Reserch Foundation, INCa, and Ligue Nationale Contre le Cancer. TG and CB received PhD grants from the Ministry of Research and Higher Education and the Fondation pour la Recherche Médicale.

AUTHOR CONTRIBUTIONS

CW performed and supervised most of the experiments and contributed to the design of the study; TD, CB, NP, CL, PR, CC, VE, NS, AS, VM, ND, CM performed experiments; LL, AA, RH and AP realized bioinformatic analyses; JLV and OAW provided mouse models; SG and FP provided experimental human samples; CW, RS, JLV, OAW, CM, IP, SNC, FP and WV analysed the data; ES designed and supervised the study and wrote the paper. All authors approved the paper.

COMPETING INTERESTS

The author declares no competing interests.

ADDITIONAL INFORMATION

Supplementary information The online version contains supplementary material available at https://doi.org/10.1038/s41375-023-01878-0.

Correspondence and requests for materials should be addressed to Eric Solary.

Reprints and permission information is available at http://www.nature.com/reprints

Publisher's note Springer Nature remains neutral with regard to jurisdictional claims in published maps and institutional affiliations.